Termination of shoot gravitropic responses by auxin feedback on PIN3 polarity

Hana Rakusová,[1,2] Mohamad Abbas,[1] Huibin Han,[1] Siyuan Song,[1] Hélène S. Robert,[3] and Jiří Friml[1*]

[1] Institute of Science and Technology (IST) Austria, 3400 Klosterneuburg, Austria

[2] Department of Plant Systems Biology, VIB and Department of Plant Biotechnology and Bioinformatics, Ghent University, 9052 Gent, Belgium

[3] Mendel Centre for Plant Genomics and Proteomics, Masaryk University, CEITEC MU, 625 00 Brno, Czech Republic

[*] Correspondence: jiri.friml@ist.ac.at

SUMMARY

Plants adjust their growth according to gravity. Gravitropism involves gravity perception, signal transduction, and asymmetric growth response, with organ bending as a consequence [1]. Asymmetric growth results from the asymmetric distribution of the plant-specific signaling molecule auxin [2] that is generated by lateral transport, mediated in the hypocotyl predominantly by the auxin transporter PIN-FORMED3 (PIN3) [3-5]. Gravity stimulation polarizes PIN3 to the bottom sides of endodermal cells, correlating with increased auxin accumulation in adjacent tissues at the lower side of the stimulated organ, where auxin induces cell elongation and, hence, organ bending. A curvature response allows the hypocotyl to resume straight growth at a defined angle [6], implying that at some point auxin symmetry is restored to prevent overbending. Here, we present initial insights into cellular and molecular mechanisms that lead to the termination of the tropic response. We identified an auxin feedback on PIN3 polarization as underlying mechanism that restores symmetry of the PIN3-dependent auxin flow. Thus, two mechanistically distinct PIN3 polarization events redirect auxin fluxes at different time points of the gravity response: first, gravity-mediated redirection of PIN3-mediated auxin flow towards the lower hypocotyl side, where auxin gradually accumulates and promotes growth, and later PIN3 polarization to the opposite cell side, depleting this auxin maximum to end the bending. Accordingly, genetic or pharmacological interference with the late PIN3 polarization prevents termination of the response and leads to hypocotyl overbending. This observation reveals a role of auxin feedback on PIN polarity in the termination of the tropic response.

RESULTS AND DISCUSSION

Auxin distribution and PIN3 polarization during gravity response in *Arabidopsis thaliana* hypocotyls

To describe the gravitropic response of etiolated *Arabidopsis thaliana* hypocotyls, we analyzed their bending kinetics. The initial bending starts after 2-3 h of 90º gravistimulation; it diminishes after approximately 18 h and stops after approximately 30 h (Figure 1A). Auxin fluxes and accumulation were indirectly monitored based on the expression pattern of the auxin transporter PIN3-GFP and of the auxin signaling reporters *p35S::DII-VENUS* and *pDR5rev::GFP* at various time points (Figure S1). We detected a pronounced DII-VENUS and *pDR5rev::GFP* signal asymmetry after 4 h and 6 h of gravistimulation, respectively (Figures 1B, 1G, and 1J). At approximately 36 h, DII-VENUS and *pDR5rev::GFP* signals across the hypocotyl became symmetrical again (Figures 1H and 1K). As described previously [3], PIN3-GFP, initially localized symmetrically at the plasma membrane (PM) of endodermal cells, relocated to the bottom PM after 2 h of gravistimulation (Figures 1B-1D). Notably, after 24 h, PIN3-GFP at the lower hypocotyl side disappeared from the outer/bottom PM and remained only in the inner/upper PM of the endodermal cells (Figures 1B and 1E).

In summary, we observed two distinct PIN3 polarization events that were followed by changes in the spatial pattern of the auxin response during hypocotyl gravitropism. Initially, the symmetrically localized PIN3 polarizes to the bottom PM of the endodermal cells followed by an increased auxin response in the adjacent cells at the lower hypocotyl side. Later on, at the lower organ side with high auxin response, PIN3 relocates from the bottom to the upper PM, reestablishing the symmetrical localization between the upper and lower sides of the hypocotyl. Subsequently, the even auxin response is restored across the organ and the bending ends.

Auxin feedback-mediated PIN3 polarization in hypocotyl endodermis

Auxin moves among cells in a directional manner that depends on the polarized localization of the PIN transporters at the PM [7]. Therefore, changes in the PIN polarity can redirect auxin fluxes. Indeed, the two PIN3 polarization events observed during hypocotyl gravitropism correlated with the subsequent changes in the asymmetric auxin response distribution (Figure 1). As the first PIN3 polarization event follows gravity perception and downstream signalling [3], we assessed how the second PIN3 polarization event is mediated.

Feedback regulation of the PIN polarity by auxin itself has been proposed to underlie a self-organizing tissue polarization [8, 9]. Therefore, given that the second PIN3 polarization occurs specifically at the lower organ side, where auxin accumulates during the gravitropic response, we tested the role of auxin in this process. First, we examined whether auxin accumulation at the lower hypocotyl side is required for this PIN3 polarization. We pretreated *pPIN3::PIN3-GFP p35S::DII-VENUS* seedlings with the auxin transport inhibitor *N*-(1-naphtyl)phtalamic acid (NPA) for 2 h, where after the seedlings were gravistimulated for 8 h. Under these conditions, the first, gravity-mediated PIN3-GFP polarization occurred normally (Figures S2H-S2L), but, because the auxin transport was inhibited by NPA, the DII-VENUS gradient was not established. Furthermore, PIN3 retained its gravity-induced asymmetrical localization, even when NPA was applied 16 h after the beginning of the gravistimulation and analyzed after continued gravistimulation for another 8 h (Figures 2A-2F). Thus, when a prolonged auxin accumulation at the lower hypocotyl side is prevented, the second PIN3 polarization event does not occur.

Next, we treated etiolated seedlings with natural and synthetic auxins, namely indole-3-acetic acid (IAA) and naphthalene-1-acetic acid (NAA), respectively. Auxin treatments induced similar changes in PIN3-GFP localization to the inner PM of endodermal cells of

hypocotyls, i.e. “inner-lateralization” as observed at the place of endogenous auxin accumulation at the hypocotyl lower side (Figures 2G-2J, S2C-S2D). Measurement of the PIN3-GFP fluorescence intensity ratio between the inner-lateral and the outer-lateral endodermal PM revealed that exogenous auxin, in a time and concentration-dependent manner, caused PIN3 inner-lateralization (Figures 2J; S2A-S2E; see Experimental procedures). Exogenous auxin application also affected hypocotyl bending. Low concentrations stimulated bending, causing slight hyperbending responses and high concentrations were inhibitory, correlating with cell elongation inhibition in general (Figures S2F and S2G).

Next, we examined whether the auxin effect on the PIN localization was specific to PIN3. We tested *pPIN7::PIN7-GFP*, because PIN7 is also expressed in the hypocotyl [3], and *pSCR::PIN2-GFP* that expresses PIN2 specifically in the endodermis. PIN7 and PIN2 both relocated to the inner-lateral PM after auxin treatment, similarly to PIN3-Y/GFP (Figures S2M, S2R-S2T), indicating that the auxin effect is not specific to a particular PIN protein. Additionally, the use of the *SCARECROW* (*SCR*) promoter confirmed that gravity- or auxin-induced PIN polarity changes are not a consequence of their influence on the PIN transcription. We also used another integral PM protein marker (*pUBQ10::Wave131-YFP*). After gravity stimulation or auxin application, no important significant changes in the Wave131-YFP localization were detected (Figures S3A-S3D), confirming the specificity of the gravity- and auxin-mediated polarity changes for PIN proteins. Thus, increased auxin levels induced inner-lateralization of PIN proteins in hypocotyl endodermal cells, providing a plausible mechanism for the second PIN3 polarization event that reestablishes the symmetrical PIN3 localization at later stages of tropic responses in hypocotyls.

Vacuolar targeting and protein degradation in auxin-induced PIN3 polarization

PIN3-GFP fluorescence intensity measurements revealed that after gravistimulation the signal decreased from the outer and increased in the inner PM of the cells at the upper hypocotyl sidel (Figures S1J, S3E). Thus, for the gravity-induced polarization, PIN3 might translocate from the outer to the inner PM by the so-called transcytosis mechanism, similar to that shown for roots [10]. In contrast, auxin treatment decreased the PIN3-GFP signal at the outer-lateral side, but did not substantially increase it at the inner-lateral side (Figure S3E), suggesting a contribution of the PIN3 degradation during the auxin-mediated PIN3 polarization. We tested whether protein synthesis played a role by using cycloheximide (CHX) treatment and degradation with MG132 in the auxin-induced PIN3 inner-lateralization. CHX blocks protein synthesis and inhibits growth of hypocotyls [3]. After cotreatment with NAA, the PIN3-GFP inner-lateralization was normal (Figures S3F-S3H). These data indicate that the auxin effect on the PIN3 polarization does not depend on *de novo* protein synthesis. The treatment with MG132, a drug blocking proteasome function and PIN degradation [11], did not affect the gravity-induced PIN3 polarization [3], but it reduced the auxin-mediated PIN3 polarization (Figures S3I-S3K). This observation implies that the protein degradation contributes to the auxin-induced PIN3 inner-lateralization. Auxin controls the PIN protein abundance by promoting the vacuolar targeting and degradation as part of the gravitropic response in roots [12, 13]. To characterize whether the protein degradation via vacuolar targeting is needed for the PIN3 polarization, we examined the effect of wortmannin (WM), an inhibitor of PIN trafficking to the vacuole [12]. WM did not influence the gravity bending response (Figures S3L-S3N), only reduced slightly the gravity-induced PIN3-GFP polarization (Figures S3O-S3Q), but interfered extensively with PIN3-GFP polarization after auxin treatment, as manifested by a persistent PIN3-GFP localization at the outer-endodermal cell sides (Figures S4A-S4C). These data suggest a role for vacuolar trafficking and degradation during the auxin-mediated PIN3 polarization, but not in the gravity-induced polarization.

Clathrin-mediated endocytosis and GNOM-dependent recycling in auxin-induced PIN3 polarization

Next, we assessed the contribution of trafficking processes to the auxin-mediated PIN3 polarization [3]. PIN proteins constitutively cycle between the PM and the endosomal compartments [14]. These subcellular dynamics require clathrin-mediated endocytosis [15, 16] and GNOM ARF GEF-dependent recycling [17].

To test a possible role of clathrin during the PIN3 polarization, we used tyrphostin A23 (Tyr23) [18] to interfere with the PIN internalization [15]. Tyr23 blocked both gravity- and auxin-mediated PIN3-GFP polarization in endodermal cells (Figures S4D-S4K). In addition, we tested the *pINTAM>>RFP-HUB1* line that conditionally expresses the C-terminal part of the clathrin heavy chain (termed HUB1) and exerts dominant negative effects on the clathrin function [19]. This interference with clathrin inhibited the gravity-induced PIN3-GFP polarization (Figures S4L-S4N) as well as the auxin-induced PIN3-GFP inner-lateralization (Figures 3A-3E). Moreover, we examined whether the auxin-mediated PIN3 polarization requires GNOM-dependent vesicular trafficking as previously shown for the gravity-induced PIN3 polarization [3]. When seedlings were treated with brefeldin A (BFA), a fungal drug inhibiting a subclass of ARF–GEFs, including GNOM, and then treated together with BFA+NAA, PIN3-GFP remained at the outer PM without inner-lateralization (Figures 3F and 3I). The inhibitory effect of BFA on the auxin-induced PIN3-GFP inner-lateralization was largely rescued in a transgenic line carrying a $GNOM^{M696L}$ version resistant to BFA (Figures 3G-3I), These experiments revealed the importance of clathrin and GNOM ARF GEF activities for both gravity- and auxin-induced PIN3 polarizations.

The ability of Tyr23 to interfere with PIN3 polarizations allowed us to time its effect and, thus, to interfere specifically with the second auxin-mediated PIN3 polarization in the

course of the gravitropic response. *pPIN3::PIN3-GFP p35S::DII-VENUS* seedlings were subjected to gravity stimulation for 16 h and then moved carefully to preserve orientation and gravity stimulation on Tyr23-containing medium for another 8 h (Figure 3J–3L). Indeed, in this configuration, Tyr23 stabilized PIN3-GFP at the bottom side of the endodermal cells, preventing its auxin-induced polarization, which occurred when seedlings were moved to control medium (Fig. 3M). Notably, when PIN3 remained at the bottom cell sides, also the DII-VENUS--monitored auxin asymmetry did not disappear as seen in controls (Fig. 3N) and the hypocotyls overbent (Fig. 3O). Thus, these observations indicate that when PIN3-GFP polarization is prevented at later stages of the gravity response, the auxin asymmetry persists, leading to hypocotyl overbending.

PINOID-mediated phosphorylation for auxin-induced PIN3 polarization

PIN phosphorylation by the serine/threonine protein kinase PINOID (PID) is one of the key mechanisms in the PIN polarity regulation [20-22]. We tested whether phosphorylation by PID contributes to the auxin-mediated PIN3 polarization. The *PID* overexpressor line *35S::PID* was defective in the auxin-mediated PIN3-GFP polarization (Figures S4O-S4Q), similarly to the gravity-induced PIN3 polarization [3]. As a consequence, *35S::PID* seedlings displayed an altered gravitropic response (Figures 4E and 4G), showing that ectopically increased PID activity can overrule both the gravity- and auxin-mediated control of the PIN3 polarization, thus interfering with both polarizations.

We also tested the *wag1 wag2 pid* triple mutant that lacks activity of PID and of its two closest homologues [23]. In this triple mutant, the PIN3-GFP signal was weaker and the inner-lateral PIN3-GFP polarization appeared more pronounced, but treatment with auxin did not lead to further PIN3-GFP polarizations (Figures S4R and S4T). We tested this line directly in the context of the gravitropic response. The gravity-induced PIN 3 polarization of the *wag1*

wag2 pid triple mutant was normal (Fig. 4A), but the second polarization event was defective as demonstrated by the persistence of PIN3-GFP at the bottom sides of endodermal cells, even 16 h or 24 h after gravistimulation (Fig. 4A-4D). Thus, this line genetically separated the two PIN3 polarization events and allowed assessment of their role in gravitropic bending. Notably, the failure of the *wag1 wag2 pid* triple mutant to execute the second PIN3 polarization in response to auxin correlated with the overbending growth response (Figure 4E-4H).

Taken together, PID-dependent phosphorylation seems to be required, not for the gravity-mediated, but more specifically, for the auxin-mediated PIN3 polarization. Overbending of this line confirms the importance of this process for the termination of the gravitropic response.

CONCLUSIONS

The mechanisms underlying plant gravitropism have been extensively studied over the last century. Whereas gravity perception and initiation of growth responses are relatively well understood, virtually nothing is known about how plants terminate the response to prevent overbending. Our observations revealed two separate PIN3 polarization events in hypocotyl endodermal cells during the gravitropic response: (*i*) the early gravity-induced polarization to the bottom PM [3] and (*ii*) the later, auxin-dependent PIN3 polarization to the inner (upper) PM at the lower organ side. These subsequent polarizations are consistent with the initial auxin flow towards the lower side, where auxin accumulates. Then, the auxin flow reverses from the lower side, equalizing the auxin levels between the lower and upper sides and the onset of the symmetric shoot growth. Our data suggest that the second PIN3 polarization depends on the feedback from the auxin accumulated at the lower organ side. Indeed, when auxin accumulation was impeded by auxin transport inhibition, the gravity-induced PIN3 polarization occurred

normally, but the second polarization was prevented. In addition, exogenous auxin to nonstimulated hypocotyls was sufficient to induce similar PIN3 polarizations.

The PIN3 polarization in response to gravity [3] or to auxin requires partially overlapping, but distinct, cellular processes. Similar to the gravity-induced PIN3 polarization, the auxin-mediated polarization also needs clathrin-mediated endocytosis, GNOM ARF GEF-dependent PIN recycling, and PID kinase-dependent PIN phosphorylation regulatory circuits. Notably, a specific interference with the auxin-mediated PIN3 polarization, either genetic or pharmacological, leads to the overbending response, strongly implying that this feedback-mediated reestablishment of the symmetrical localization of PIN3 provides a mechanism for the previously unexplained process of bending termination during tropic responses.

SUPPLEMENTAL INFORMATION

Supplemental Information includes Experimental procedure and four Figures and can be found with this article online.

AUTHOR CONTRIBUTIONS

H.R., M.A., H.H., S.S., H.S.R., and J.F. designed and conducted experiments and analyzed data. H.R. and J.F. wrote the manuscript, with the assistance of M.A. and H.S.R.

ACKNOWLEDGEMENTS

We thank Dr. Jie Li (Key Laboratory of Plant Molecular Physiology, Chinese Academy of Science, China) for the *pPIN3::PIN3-GFP/DII::VENUS* line and Martine De Cock for help in preparing the manuscript. This work was supported by the European Research Council (project ERC-2011-StG-20101109-PSDP); European Social Fund (CZ.1.07/2.3.00/20.0043) and the

Czech Science Foundation GAČR (GA13-40637S) to J.F. and H.S.R. H.R. is indebted to the Agency for Innovation by Science and Technology (IWT) for a predoctoral fellowship.

COMPETING FINANCIAL INTEREST

The authors declare no competing financial interests.

REFERENCES

1. Bastien, R., Bohr, T., Moulia, B., and Douady, S. (2013). Unifying model of shoot gravitropism reveals proprioception as a central feature of posture control in plants. Proc. Natl. Acad. Sci. USA *110*, 755-760.
2. Hashiguchi, Y., Tasaka, M., and Morita, M.T. (2013). Mechanism of higher plant gravity sensing. Am. J. Bot. *100*, 91-100.
3. Rakusová, H., Gallego-Bartolome, J., Vanstraelen, M., Robert, H.S., Alabadi, D., Blazquez, M.A., Benková, E., and Friml, J. (2011). Polarization of PIN3-dependent auxin transport for hypocotyl gravitropic response in *Arabidopsis thaliana*. Plant J. *67*, 817-826.
4. Friml, J., Wiśniewska, J., Benková, E., Mendgen, K., and Palme, K. (2002). Lateral relocation of auxin efflux regulator PIN3 mediates tropism in *Arabidopsis*. Nature *415*, 806-809.
5. Ding, Z., Galvan-Ampudia, C.S., Demarsy, E., Łangowski, Ł., Kleine-Vehn, J., Fan, Y., Morita, M.T., Tasaka, M., Fankhauser, C., Offringa, R., et al. (2011). Light-mediated polarization of the PIN3 auxin transporter for the phototropic response in *Arabidopsis*. Nat. Cell Biol. *13*, 447-452.
6. Masson, P.H., Tasaka, M., Morita, M.T., Guan, C., Chen, R., and Boonsirichai, K. (2002). *Arabidopsis thaliana*: A model for the study of root and shoot gravitropism. The Arabidopsis Book *1*, e0043.
7. Adamowski, M., and Friml, J. (2015) PIN-dependent auxin transport: action, regulation, and evolution. Plant Cell. *27*, 20-32.

8. Wabnik, K., Kleine-Vehn, J., Balla, J., Sauer, M., Naramoto, S., Reinöhl, V., Merks, R.M.H., Govaerts, W., and Friml, J. (2010). Emergence of tissue polarization from synergy of intracellular and extracellular auxin signaling. Mol. Syst. Biol. *6*, 447.

9. Sauer, M., Balla, J., Luschnig, C., Wiśniewska, J., Reinöhl, V., Friml, J., and Benková, E. (2006). Canalization of auxin flow by Aux/IAA-ARF-dependent feedback regulation of PIN polarity. Genes Dev. *20*, 2902-2911.

10. Kleine-Vehn, J., Ding, Z., Jones, A.R., Tasaka, M., Morita, M.T., and Friml, J. (2010). Gravity-induced PIN transcytosis for polarization of auxin fluxes in gravity-sensing root cells. Proc. Natl. Acad. Sci. USA *107*, 22344-22349.

11. Abas, L., Benjamins, R., Malenica, N., Paciorek, T., Wiśniewska, J., Moulinier-Anzola, J.C., Sieberer, T., Friml, J., and Luschnig, C. (2006). Intracellular trafficking and proteolysis of the *Arabidopsis* auxin-efflux facilitator PIN2 are involved in root gravitropism. Nat. Cell Biol. *8*, 249-256.

12. Kleine-Vehn, J., Leitner, J., Zwiewka, M., Sauer, M., Abas, L., Luschnig, C., and Friml, J. (2008). Differential degradation of PIN2 auxin efflux carrier by retromer-dependent vacuolar targeting. Proc. Natl. Acad. Sci. USA *105*, 17812-17817.

13. Baster, P., Robert, S., Kleine-Vehn, J., Vanneste, S., Kania, U., Grunewald, W., De Rybel, B., Beeckman, T., and Friml, J. (2013). $SCF^{TIR1/AFB}$-auxin signalling regulates PIN vacuolar trafficking and auxin fluxes during root gravitropism. EMBO J. *32*, 260-274.

14. Geldner, N., Friml, J., Stierhof, Y.-D., Jürgens, G., and Palme, K. (2001). Auxin transport inhibitors block PIN1 cycling and vesicle trafficking. Nature *413*, 425-428.

15. Dhonukshe, P., Aniento, F., Hwang, I., Robinson, D.G., Mravec, J., Stierhof, Y.-D., and Friml, J. (2007). Clathrin-mediated constitutive endocytosis of PIN auxin efflux carriers in *Arabidopsis*. Curr. Biol. *17*, 520-527.

16. Kitakura, S., Vanneste, S., Robert, S., Löfke, C., Teichmann, T., Tanaka, H., and Friml, J. (2011). Clathrin mediates endocytosis and polar distribution of PIN auxin transporters in *Arabidopsis*. Plant Cell *23*, 1920-1931.

17. Geldner, N., Anders, N., Wolters, H., Keicher, J., Kornberger, W., Muller, P., Delbarre, A., Ueda, T., Nakano, A., and Jürgens, G. (2003). The *Arabidopsis* GNOM ARF-GEF mediates endosomal recycling, auxin transport, and auxin-dependent plant growth. Cell *112*, 219-230.

18. Dejonghe, W., Kuenen, S., Mylle, E., Vasileva, M., Keech, O., Viotti, C., Swerts, J., Fendrych, M., Ortiz-Morea, F.A., Mishev, K. et al. (2016). Mitochondrial uncouplers inhibit clathrin-mediated endocytosis largely through cytoplasmic acidification. Nat. Commun. *7*, 11710.

19. Robert, S., Kleine-Vehn, J., Barbez, E., Sauer, M., Paciorek, T., Baster, P., Vanneste, S., Zhang, J., Simon, S., Čovanová, M., et al. (2010). ABP1 mediates auxin inhibition of clathrin-dependent endocytosis in *Arabidopsis*. Cell *143*, 111-121.

20. Zhang, J., Nodzyński, T., Pěnčik, A., Rolčik, J., and Friml, J. (2010). PIN phosphorylation is sufficient to mediate PIN polarity and direct auxin transport. Proc. Natl. Acad. Sci. USA *107*, 918-922.

21. Friml, J., Yang, X., Michniewicz, M., Weijers, D., Quint, A., Tietz, O., Benjamins, R., Ouwerkerk, P.B.F., Ljung, K., Sandberg, G., et al. (2004). A PINOID-dependent binary switch in apical-basal PIN polar targeting directs auxin efflux. Science *306*, 862-865.

22. Huang, F., Kemel Zago, M., Abas, L., van Marion, A., Galvan-Ampudia, C.S., and Offringa, R. (2010). Phosphorylation of conserved PIN motifs directs *Arabidopsis* PIN1 polarity and auxin transport. Plant Cell *22*, 1129-1142.

23. Santner, A.A., and Watson, J.C. (2006). The WAG1 and WAG2 protein kinases negatively regulate root waving in Arabidopsis. Plant J. *45*, 752-764.

24. Žádníková, P., Petrášek, J., Marhavý, P., Raz, V., Vandenbussche, F., Ding, Z., Schwarzerová, K., Morita, M.T., Tasaka, M., Hejátko, J., et al. (2010). Role of PIN-mediated auxin efflux in apical hook development of *Arabidopsis thaliana*. Development *137*, 607-617.

25. Blilou, I., Xu, J., Wildwater, M., Willemsen, V., Paponov, I., Friml, J., Heidstra, R., Aida, M., Palme, K., and Scheres, B. (2005). The PIN auxin efflux facilitator network controls growth and patterning in *Arabidopsis* roots. Nature *433*, 39-44.

26. Xu, J., Hofhuis, H., Heidstra, R., Sauer, M., Friml, J., and Scheres, B. (2006). A molecular framework for plant regeneration. Science *311*, 385-388.

27. Geldner, N., Denervaud-Tendon, V., Hyman, D.L., Mayer, U., Stierhof, Y.-D., and Chory, J. (2009). Rapid, combinatorial analysis of membrane compartments in intact plants with a multicolor marker set. Plant J. *59*, 169-178.

28. Friml, J., Vieten, A., Sauer, M., Weijers, D., Schwarz, H., Hamann, T., Offringa, R., and Jürgens, G. (2003). Efflux-dependent auxin gradients establish the apical-basal axis of *Arabidopsis*. Nature *426*, 147-153.

29. Dhonukshe, P., Huang, F., Galvan-Ampudia, C.S., Mähönen, A.P., Kleine-Vehn, J., Xu, J., Quint, A., Prasad, K., Friml, J., Scheres, B., et al. (2010). Plasma membrane-bound AGC3 kinases phosphorylate PIN auxin carriers at TPRXS(N/S) motifs to direct apical PIN recycling. Development *137*, 3245-3255.

30. Benjamins, R., Quint, A., Weijers, D., Hooykaas, P., and Offringa, R. (2001). The PINOID protein kinase regulates organ development in *Arabidopsis* by enhancing polar auxin transport. Development *128*, 4057-4067.

31. Brunoud, G., Wells, D.M., Oliva, M., Larrieu, A., Mirabet, V., Burrow, A.H., Beeckman, T., Kepinski, S., Traas, J., Bennett, M.J., and Vernoux, T. (2012). A novel

sensor to map auxin response and distribution at high spatio-temporal resolution. Nature *482*, 103-106.

32. Le, J., Liu, X.-G., Yang, K.-Z., Chen, X.-L., Zou, J.-J., Wang, H.-Z., Wang, M., Vanneste, S., Morita, M., Tasaka, M., et al. (2014). Auxin transport and activity regulate stomatal patterning and development. Nat. Commun. *5*, 3090.

FIGURE LEGENDS

Figure 1. *PIN3-GFP, pDR5rev::GFP,* and *DII-VENUS* expression during gravitropic bending responses of *Arabidopsis* hypocotyls

(A) Hypocotyl bending kinetics of wild-type seedlings during gravitropic reorientation. Hypocotyl curvatures were measured every hour and the average curvatures were calculated. Values are the average of three biological replicates ($n > 10$ per time point on each replicate). Error bars represent standard errors. The microscopic picture in the right corner is a time projection of the hypocotyl bending response.

(B) Scheme depicting the *pDR5rev::GFP* at the upper/lower side of the hypocotyl and the PIN3-GFP cellular localization (at the outer/inner side of endodermal cells in the upper/lower hypocotyl side) in the bending region of the hypocotyl upon the gravity response.

(C-E) PIN3-GFP localization in hypocotyl endodermis cells after 0 h (C), 2 h (D), and 24 h (E) of gravity stimulation. PIN3-GFP was apolarly localized in the hypocotyl endodermal cells before gravity stimulation (C). Following gravistimulation, PIN3-GFP localized at the inner side of endodermal cells of the upper hypocotyl side between 2 and 18 h after stimulation (D). After prolonged stimulation, PIN3 disappeared from the outer-lateral side of the lower hypocotyl side (E). Arrowheads point the outer PM of endodermal cells.

(F-H) *pDR5rev::GFP* in hypocotyls after 0 h (F), 6 h (G), and 36 h (H) of gravity stimulation. The DR5 activity (green) showed a uniform expression level in both sides of the hypocotyl (F). The DR5 activity gradient along the gravity vector clearly visible after 6 h of gravity stimulation (G). The DR5 gradient disappeared after 36 h of gravity stimulation (H). Arrowhead points to the *pDR5rev::GFP* accumulation.

(I-K) DII-VENUS accumulation in hypocotyls after 0 h (I), 4 h (J), and 32 h (K) of gravity stimulation. The DII-VENUS signal (yellow in nuclei) is distributed equally on both sides of the hypocotyls (I), forms a gradient after 4 h of stimulation (J), which disappears after 32 h (K). For the experiment set-up and quantification, see Figure S1. Scale bars represent 50 μm.

Figure 2. Auxin-induced PIN3 polarization in hypocotyl endodermal cells

(A-C) Gravistimulated *PIN3-GFP DII-VENUS* hypocotyls treated with dimethyl sulfoxide (DMSO; control) or NPA (auxin transport inhibitor). Polarization of PIN3-GFP from the outer sides of endodermal cells of the lower hypocotyl side, but not of the upper hypocotyl side, accompanied by DII-VENUS signal disappearance due to auxin accumulation at the lower hypocotyl side after 16 h of gravity stimulation (A). After another 8 h (in total 24 h gravistimulation) PIN3-GFP polarizes from both outer sides and DII-VENUS becomes evenly distributed across the hypocotyl (B). Blocking auxin transport by NPA for 8 h after 16 h of gravity stimulation (total of 24 h of gravity stimulation) leads to DII-VENUS accumulation evenly on both hypocotyl sides and results in the PIN3-GFP persistence on the outer side of the endodermis of the lower hypocotyl side (C). The PIN3-GFP signal is at the cell surface, whereas the DII-VENUS signal is in the nuclei. Scale bars represent 50 μm. Arrowheads indicate PIN3-GFP lateralization.

(D-F) Relative PIN3-GFP and DII-VENUS signal intensities at 16 h of gravistimulation followed by 8 h of DMSO or NPA treatments. Graphs represent upper-to-lower ratio of DII-VENUS signal intensity (D and E). Mean ratio of the lower-to-upper PIN3-GFP fluorescence intensities in the outer endodermal cells sides (F). Error bars represent standard errors (Student's t test, ** $P < 0.01$; *** $P < 0.001$).

(G-J) PIN3-GFP polarization from outer-to-inner side of endodermal cells caused by auxin. After 4 h of 10 μM NAA (I) and 10 μM IAA (H and I) treatments, PIN3-GFP relocated to the

inner-lateral side as compared to the control situation (G). Arrowheads point PIN3-GFP depletion from the outer-lateral cell side. Graph represents inner-to-outer ratio of PIN3-GFP signal intensity after 4 h of treatment by DMSO, 10 μM NAA, and 10 μM IAA (I). Mean ratio of the inner-to-outer signal PIN3-GFP intensity after 10 μM IAA for the given time of treatment (J). Error bars represent standard errors (Student's *t* test, ** $P < 0.01$; *** $P < 0.001$).

For the experiment set-up and quantification, see Figure S2.

Figure 3. Clathrin, GNOM, protein degradation, and vacuolar targeting roles in auxin-mediated PIN3 polarization

(A-E) Lack of altered PIN3-GFP localization in induced *pINTAM* control (A) and induced *pINTAM>>RFP-HUB1* line (C), whereas induced *pINTAM>>RFP-HUB1* showed inhibition of the auxin effect on the PIN3-GFP inner-lateralization (D) compared to the NAA-treated induced *pINTAM* control (B). (E) Quantitative evaluation of auxin-dependent PIN3-GFP polarization. Graph shows mean ratio of inner-to-outer signal intensity. Error bars represent standard errors (Student's *t* test, * $P < 0.05$). Arrowheads point the PIN3-GFP depletion from the outer-lateral side of endodermal cells.

(F-I) Brefeldin A (BFA) affecting auxin-induced PIN3-GFP polarization in hypocotyl endodermal cells (F). NAA (G) and NAA/BFA (H) treatments in the BFA-resistant $GNOM^{M696L}$ line showed no interference with the auxin-induced PIN3-GFP inner-lateralization. PIN3-GFP fluorescence intensity ratio of the outer-to-inner side of endodermis cells of hypocotyls after BFA treatment or BFA/NAA cotreatment (I). Error bars are standard errors (Student's t-test, * $P < 0.05$; ** $P < 0.01$). Arrowheads point the PIN3-GFP depletion from the outer-lateral side of endodermal cells. Scale bars represent 20 μm.

(J-O) Gravistimulated *PIN3-GFP DII-VENUS* hypocotyls. Tyrphostin A23 (Tyr23) treatment stabilized PIN3-GFP localization and maintained DII-VENUS accumulation in the gravistimulated hypocotyl. Seedlings were gravistimulated for 16 h before being transferred to

either DMSO or Tyr23 for 8 h with continued gravistimulation. Tyr23 treatment prevented the polarization of PIN3 from the outer endodermal cell side of the lower hypocotyl side, leading to the maintenance of the DII-VENUS gradient (J-L). The PIN3-GFP signal is visible at the cell surface, whereas the DII-VENUS signal in the nuclei. (M) Quantitative evaluation of the PIN3-GFP signal at the transfer (16 h) and 8 h after the transfer. The PIN3-GFP signal intensity represents the inner-to-outer ratio of the endodermal cells at the inner and outer lateral sides of the hypocotyl. (N) Graph represents the upper-to-lower hypocotyl side ratio of the DII-VENUS signal intensity (O) Bending kinetics representing the bending angle of the hypocotyl on DMSO or Tyr23 treatment. Seedlings were gravistimulated for 16 h before transfer to Tyr23 or DMSO for the indicated time. At least 10 seedlings were measured. Error bars represent standard errors (Student's t test, * $P < 0.05$; ** $P < 0.01$; *** $P < 0.001$).

See Figures S3-S5 for a more detailed analysis of the cell specificity and the subcellular regulation of auxin- and gravity-mediated PIN3-GFP localization.

Figure 4. PINOID-mediated phosphorylation in auxin-induced PIN3 polarization

(A-D) In the triple *wag1 wag2 pid* hypocotyl mutants, PIN3-GFP polarized to the outer endodermal cell sides of the lower hypocotyl side after gravity stimulation for 6 h (A), but failed to polarize to the inner endodermal cell side of the lower hypocotyl side after 24 h (C), when compared to the control (B). Arrowheads point PIN3 depletion from the outer-lateral side of endodermal cells. Scale bars represent 20 µm. (D) Quantitative evaluation of auxin-dependent PIN3-GFP polarization in endodermis cells. Graph shows the mean ratio of lower-to-upper PIN3-GFP fluorescence intensities in the outer endodermis cell sides. Error bars represent standard errors (Student's *t* test, ** $P < 0.01$).

(E) Hypocotyl bending of wild type, *p35S::PID*, and *wag1 wag2 pid* mutants. Hypocotyl curvatures were measured after 24 h and averages were calculated. Error bars represent standard errors. Error bars represent standard errors (Student's *t* test, * $P < 0.05$; ** $P < 0.01$).

(F-H) Gravitropic response of the wild type (F), reduced bending of *p35S::PID* (G), and overbending of the *wag1 wag2 pid* mutant (H) hypocotyls. Arrowheads indicate *wag1 wag2 pid* homozygous seedlings displaying a specific phenotype, namely no developed cotyledons in dark-grown seedlings.

See Figure S4 for analysis of NAA-treated PIN3-GFP localization in *p35S::PID* and *wag1 wag2 pid* hypocotyl.

Figure 1

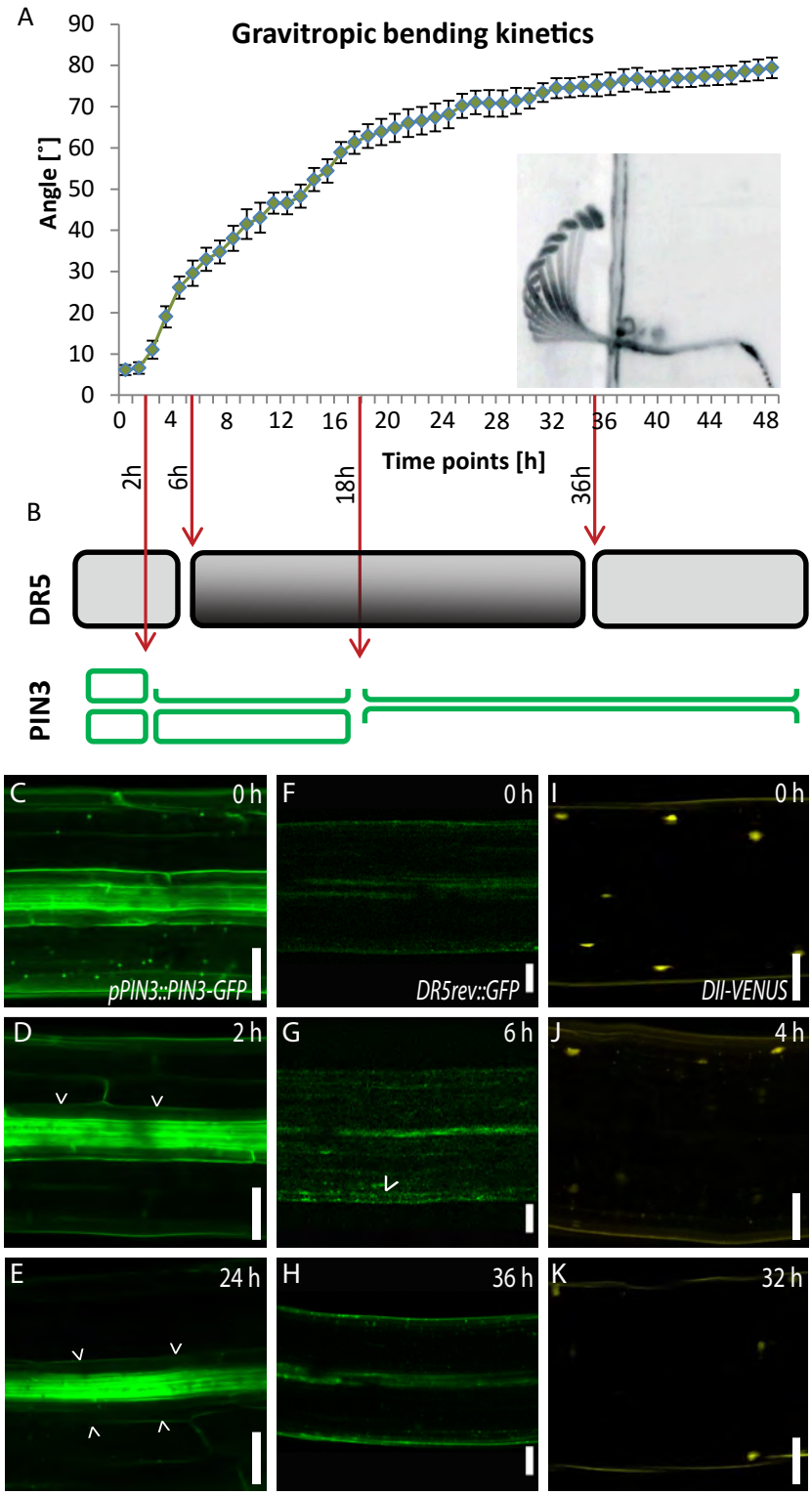
A
Gravitropic bending kinetics
Angle [°]
90
80
70
60
50
40
30
20
10
0
0
4
8
12
16
20
24
28
32
36
40
44
48
Time points [h]
2h
6h
18h
36h
B
DR5
PIN3
C
0 h
pPIN3::PIN3-GFP
F
0 h
DR5rev::GFP
I
0 h
DII-VENUS
D
2 h
G
6 h
J
4 h
E
24 h
H
36 h
K
32 h

Figure 2

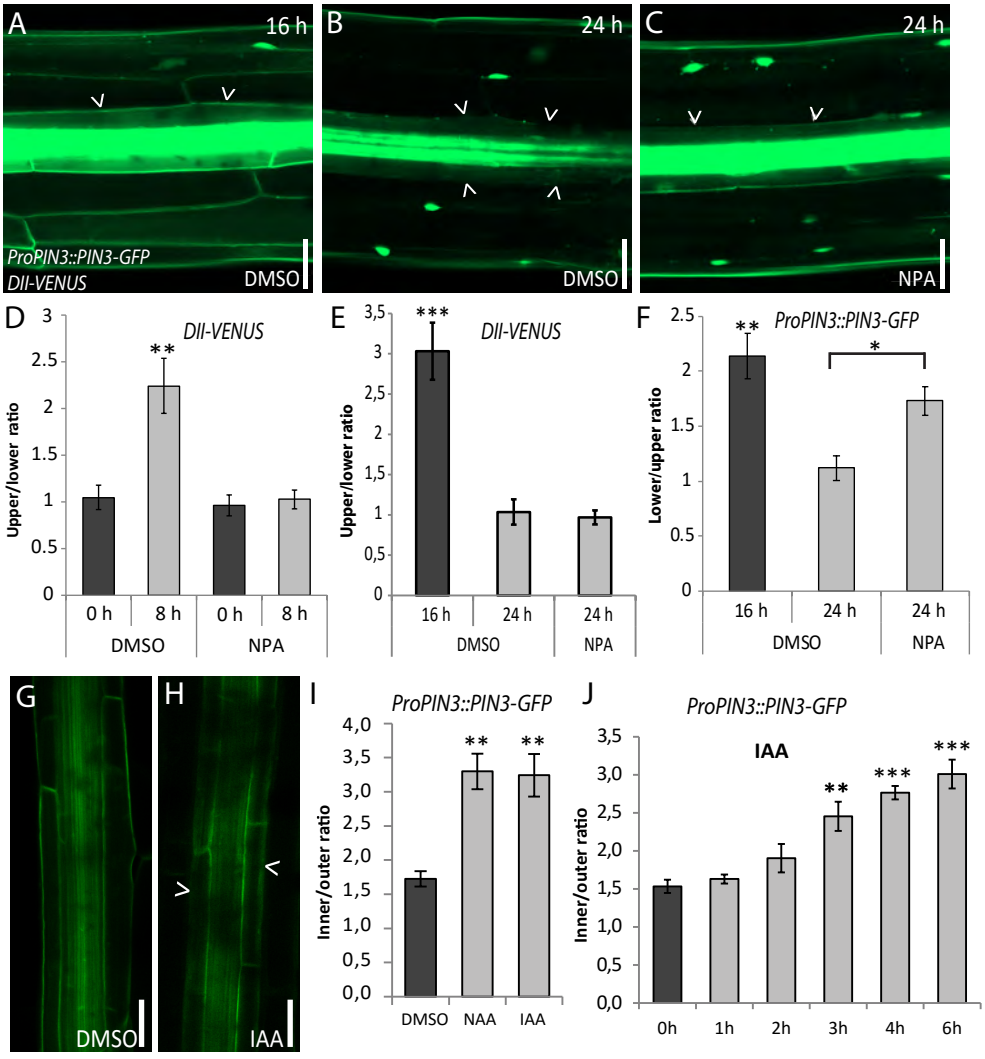
A
16 h
ProPIN3::PIN3-GFP
DII-VENUS
DMSO
B
24 h
DMSO
C
24 h
NPA
D
DII-VENUS
Upper/lower ratio
0 h
8 h
0 h
8 h
DMSO
NPA
E
DII-VENUS
Upper/lower ratio
16 h
24 h
24 h
DMSO
NPA
F
ProPIN3::PIN3-GFP
Lower/upper ratio
16 h
24 h
24 h
DMSO
NPA
G
DMSO
H
IAA
I
ProPIN3::PIN3-GFP
Inner/outer ratio
DMSO
NAA
IAA
J
ProPIN3::PIN3-GFP
IAA
Inner/outer ratio
0h
1h
2h
3h
4h
6h

Figure 3

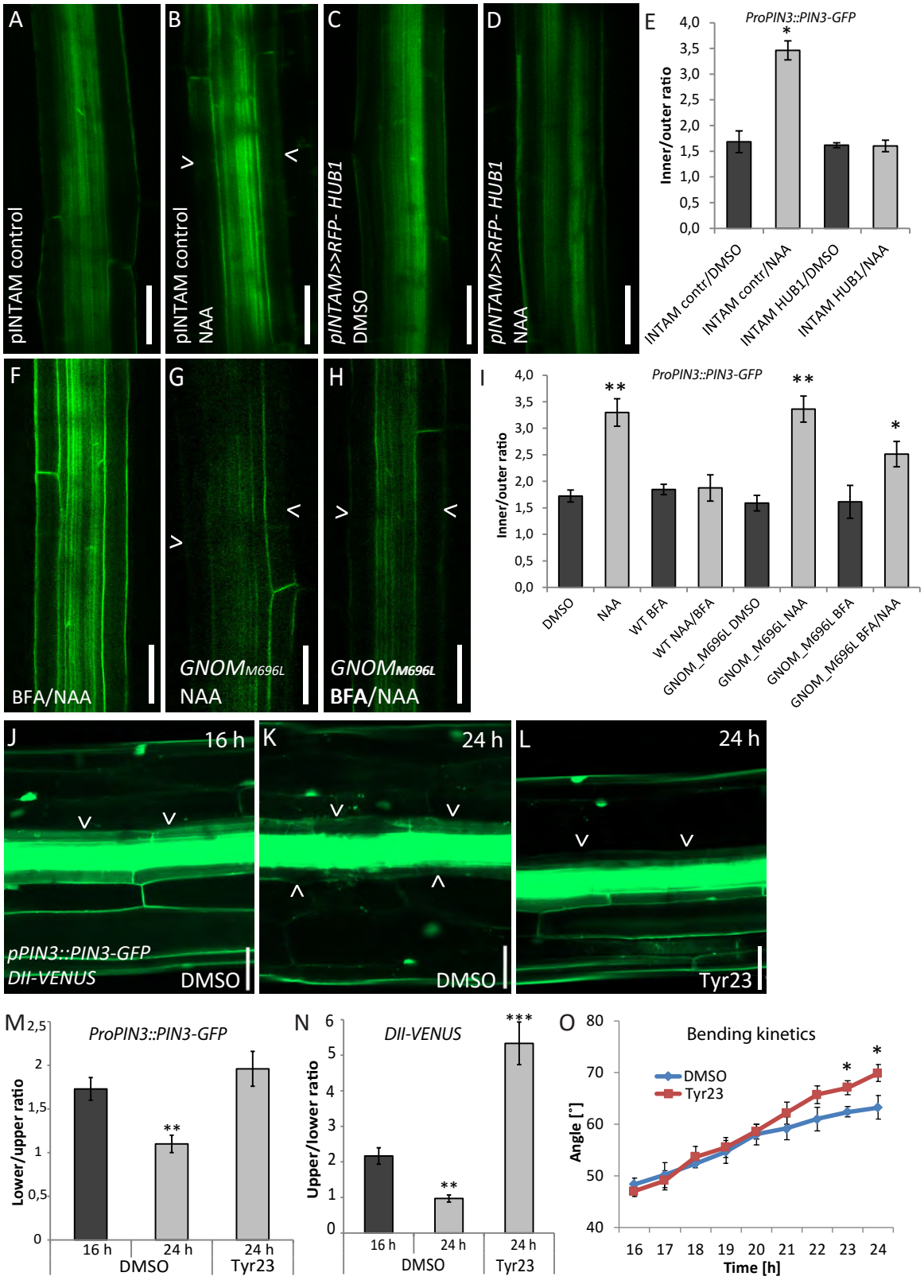
A
pINTAM control
B
pINTAM control
NAA
C
pINTAM>>RFP- HUB1
DMSO
D
pINTAM>>RFP- HUB1
NAA
E
ProPIN3::PIN3-GFP
Inner/outer ratio
4,0
3,5
3,0
2,5
2,0
1,5
1,0
0,5
0,0
*
INTAM contr/DMSO
INTAM contr/NAA
INTAM HUB1/DMSO
INTAM HUB1/NAA
F
BFA/NAA
G
GNOMM696L
NAA
H
GNOMM696L
BFA/NAA
I
ProPIN3::PIN3-GFP
Inner/outer ratio
**
**
*
DMSO
NAA
WT BFA
WT NAA/BFA
GNOM_M696L DMSO
GNOM_M696L NAA
GNOM_M696L BFA
GNOM_M696L BFA/NAA
J
16 h
pPIN3::PIN3-GFP
DII-VENUS
DMSO
K
24 h
DMSO
L
24 h
Tyr23
M
ProPIN3::PIN3-GFP
Lower/upper ratio
2,5
2
1,5
1
0,5
0
**
16 h
24 h
DMSO
24 h
Tyr23
N
DII-VENUS
Upper/lower ratio
6
5
4
3
2
1
0
***
**
16 h
24 h
DMSO
24 h
Tyr23
O
Bending kinetics
DMSO
Tyr23
Angle [°]
80
70
60
50
40
*
*
16
17
18
19
20
21
22
23
24
Time [h]

Figure 4

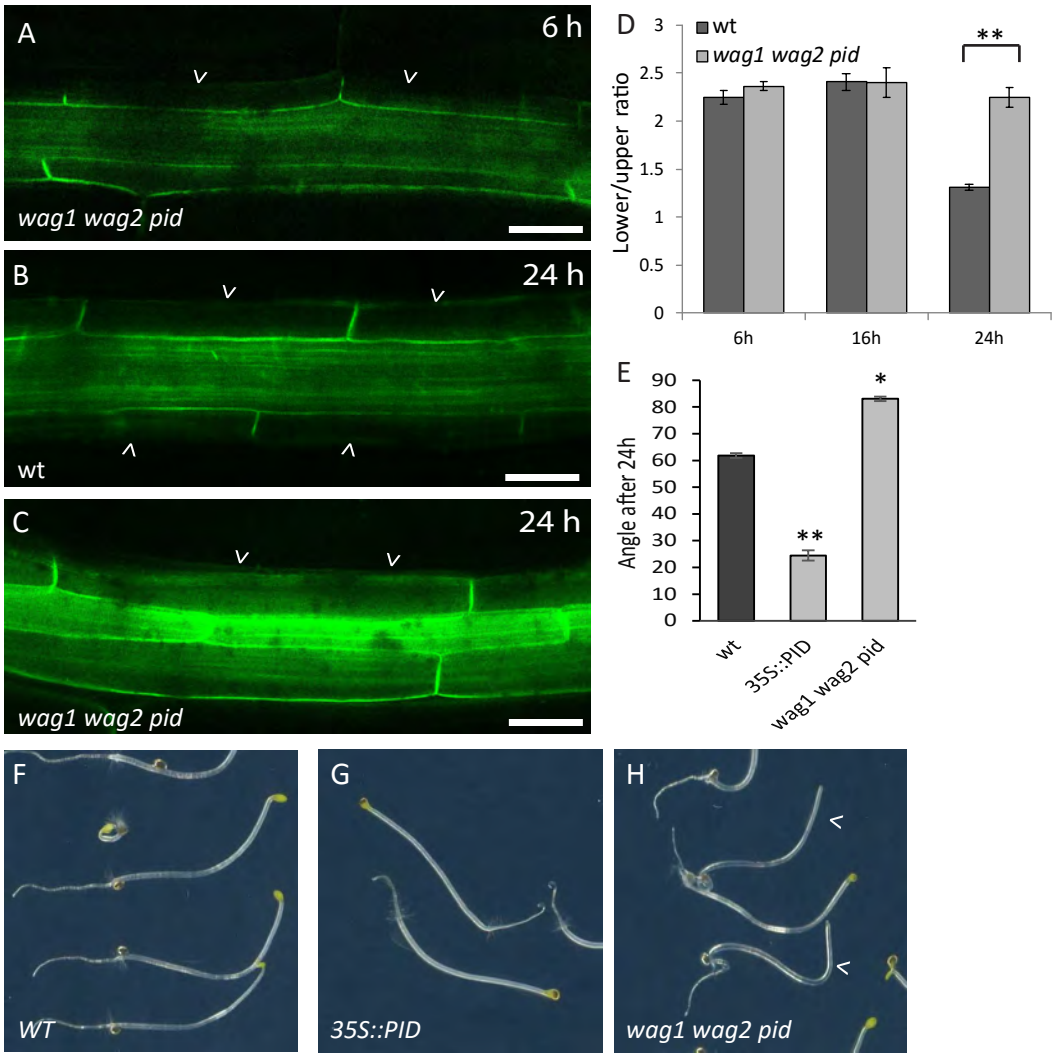
A
6 h
wag1 wag2 pid
B
24 h
wt
C
24 h
wag1 wag2 pid
D
wt
wag1 wag2 pid
Lower/upper ratio
6h
16h
24h
**
E
Angle after 24h
wt
35S::PID
wag1 wag2 pid
*
**
F
WT
G
35S::PID
H
wag1 wag2 pid

Figure S1 (Related to Figure 1 and Experimental procedures)

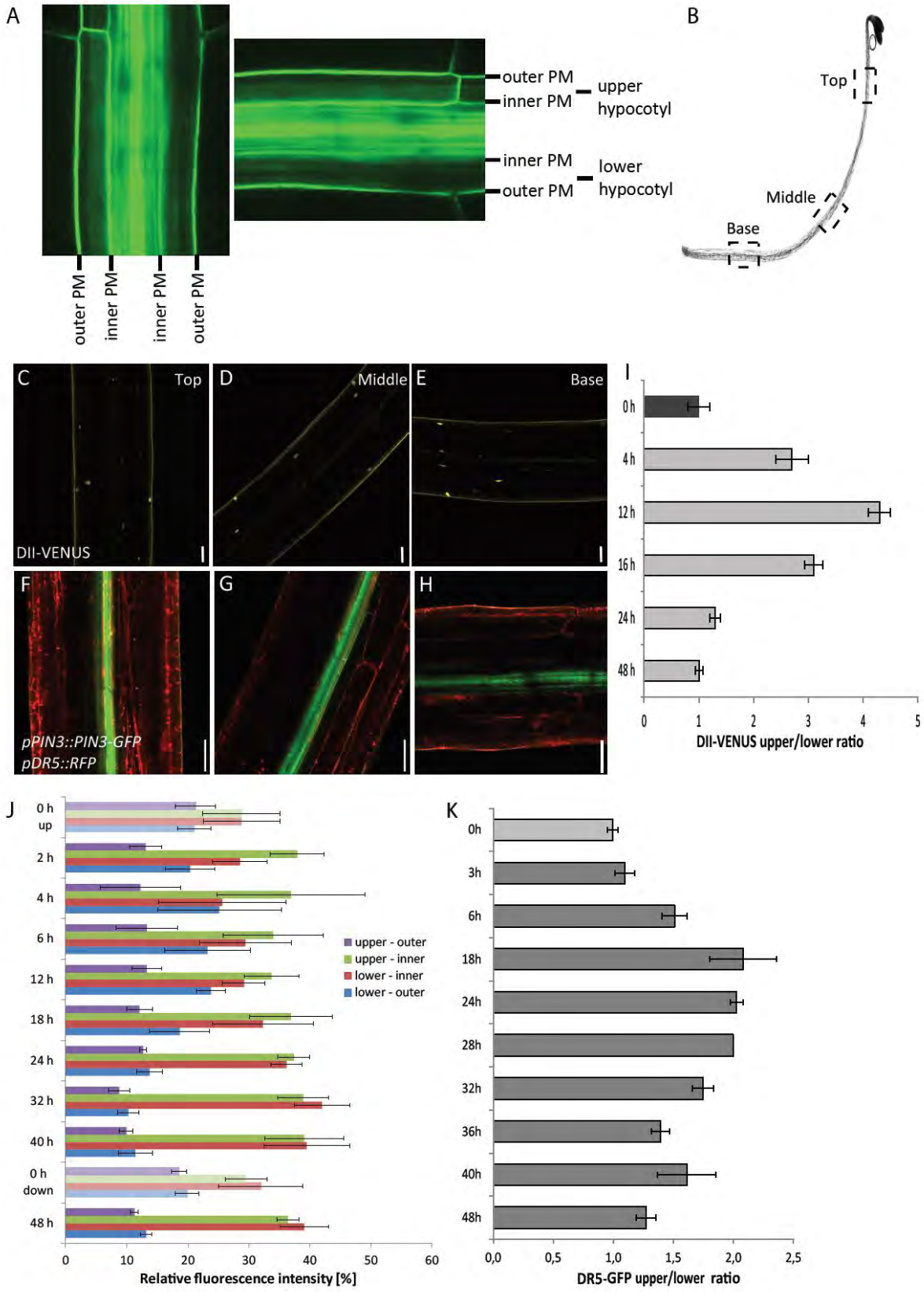

Figure S1. Evaluation of PIN3 polarity, *DR5*, and DII-VENUS changes during the hypocotyl gravity response

(A) Microscopic pictures of PIN3-GFP plasma membrane (PM) localization in hypocotyl endodermal cells in horizontal position and gravity stimulated. The nomenclature used is indicated in the text.

(B-H) Localization of PIN3-GFP, *pDR5::RFP*, and DII-VENUS in different regions of seedlings after 16 h of gravistimulation. (B) Scheme depicting a gravistimulated seedling with the positions of the three different regions of the hypocotyl (top, middle, and base) where the observations were performed (C-H). Distribution of DII-VENUS (yellow signal in nuclei) (C-E) and localization of PIN3-GFP (green signal) and *pDR5::RFP* (red signal) (F-H) in the three regions. Scale bars represent 50 μm.

(I-K) Quantification of DII-VENUS signal intensity (I), gravity-mediated PIN3 polarization (J), and *pDR5::RFP* (K) at different time points in the bended region of the gravity-stimulated hypocotyl (for instance, the middle region as depicted in B). DII-VENUS (I) and *pDR5::RFP* (K) fluorescence intensities were measured independently in the upper and lower sides of the hypocotyl. The ratio upper-to-lower for DII-Venus and lower-to-upper for *pDR5::RFP* at different time points is presented to depict the auxin response. PIN3-GFP fluorescence intensity was measured independently in outer and inner endodermis cell sides of upper and lower sides of the hypocotyl. (J) Graph representing percentage of PIN3-GFP fluorescence intensity for independent endodermis cell sides at independent time points. Error bars represent standard errors. Two control measurements at 0 h:down in the middle of the hypocotyl as control for the late time points that were measured in the bended part of the hypocotyl and up, corresponding to the nonstimulated control close to the apical hook as a control to the short gravitropic stimulations.

Figure S2 (Related to Figure 2)

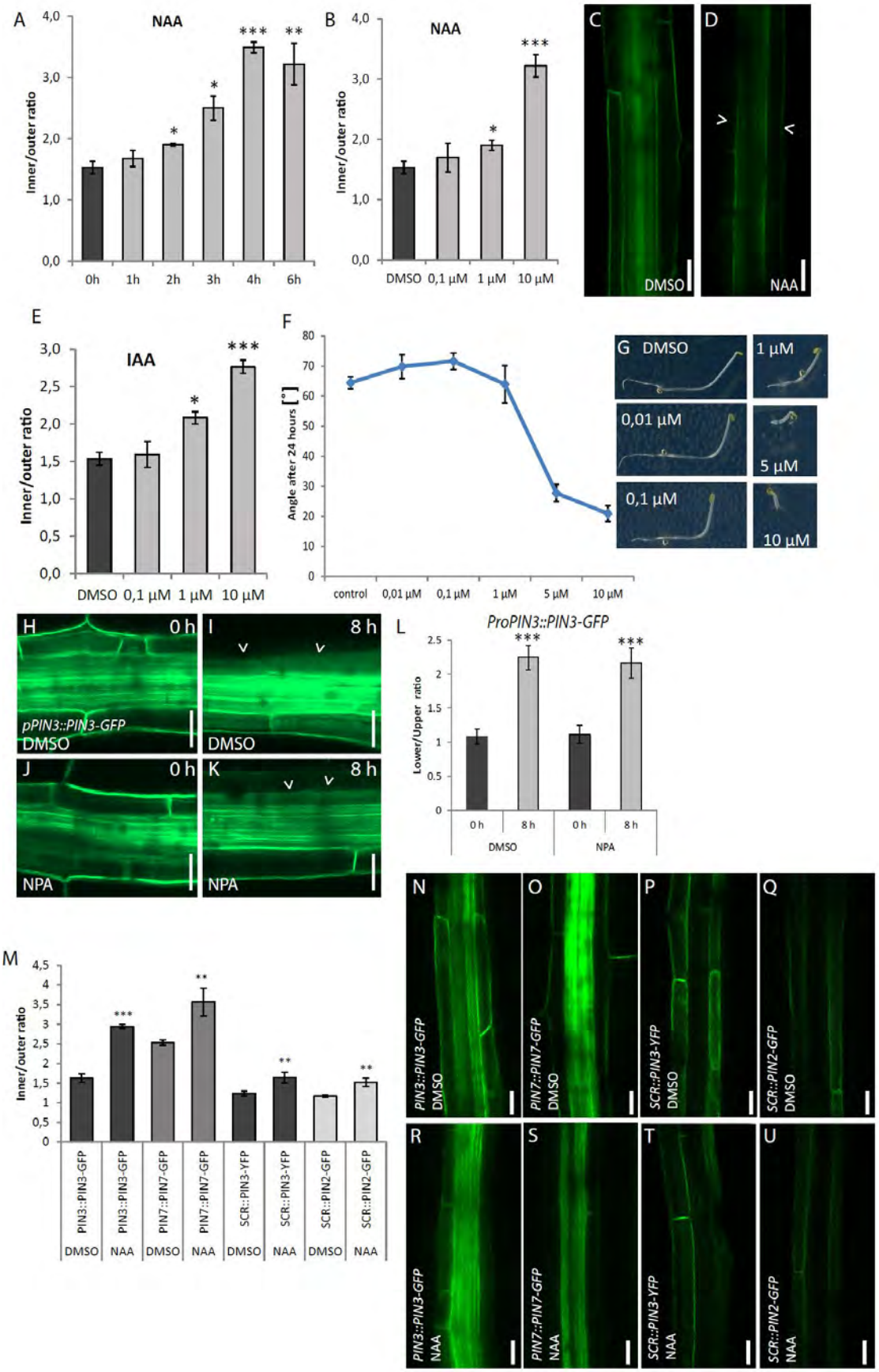

Figure S2. Auxin-dependent changes in PIN3 polarity

(A-E) Time (A) and auxin concentration (B) dependence of the PIN3-GFP lateralization with 10 μM NAA at different time points or 4 h of treatment with different NAA concentrations, respectively. After NAA treatment, the PIN3-GFP signal is reduced in the outer endodermis plasma membrane (D) compared to the DMSO-treated control (C). (E) Concentration-dependent effect of 4-h IAA treatment on the PIN3-GFP inner lateralization. Graphs show mean ratio of inner-to-outer signal intensity. Error bars represent standard errors (Student's *t* test, * $P < 0.05$; ** $P < 0.01$; *** $P < 0.001$).

(F and G) Induction of hyperbending response at low NAA concentrations. In contrast, high auxin concentration inhibits the cell elongation and reduces the bending response. Representative pictures of seedlings 24 h after gravity stimulation at given NAA concentrations (G). Graph shows the hypocotyl angle after 24 h of gravity stimulation at different concentration of NAA (F). Error bars represent standard errors.

(H-L) Pretreatment of seedlings with NPA for 8 h has no effect on gravity-induced PIN3-GFP polarization on the upper side of the hypocotyl (K) compared to the control on DMSO and NPA treatments (H and I), and not gravity-stimulated seedlings (J). Arrowheads point to PIN3-GFP depletion from outer lateral side of endodermal cells. Scale bars represent 50 μm. (L) Quantification of PIN3-GFP intensity in the upper and lower regions of the hypocotyl. Graph represents the lower-to-upper ratio of intensity. Error bars represent standard errors (Student's *t* test, *** $P < 0.001$).

(M) Quantitative evaluation of auxin-dependent PIN3-GFP, PIN7-GFP, PIN3-YFP and PIN2-GFP polarization in endodermis cells. Graph shows mean ratio of inner-to-outer signal intensity. Error bars represent standard errors (Student's t test, ** $P < 0.01$; *** $P < 0.001$).

(N-U) Effect of auxin treatment on PIN3-GFP (R), PIN7-GFP (S), PIN3-YFP (T), and PIN2-GFP (U) localization in hypocotyl endodermis compared to untreated controls (N-Q).

proSCR::PIN3-YFP (P and T) was used here as control for *proSCR::PIN2-GFP* (Q and U), where the expression is specifically in endodermal cells. Arrowheads point to PINx-G/YFP depletion from the outer lateral side of endodermal cells. Scale bars represent 20 μm.

Figure S3 (Related to Figure 3)

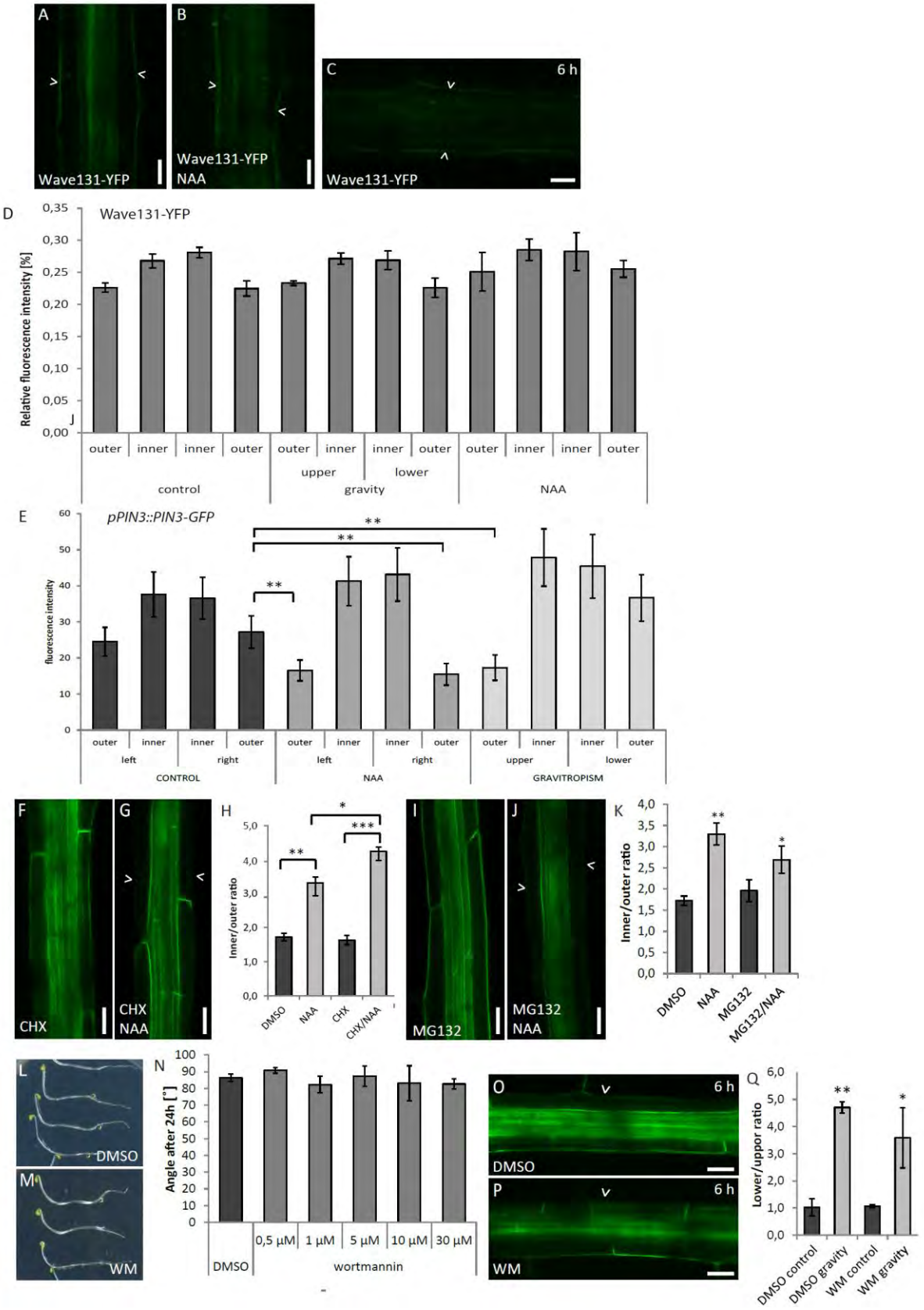

Figure S3. Cell-specific auxin effect on PIN inner-lateralization and role of protein synthesis and degradation during gravity- and auxin-mediated PIN3 polarity changes

(A-D) No polarity changes in endodermal cells of the plasma membrane (PM) marker *proUBQ10::Wave131-YFP* after 4 h of NAA treatment (B) and 6 h of gravity stimulation (C) compared to the control situation (A). Arrowheads point to the outer PM of endodermal cells. Scale bar represents 20 µm. (D) Quantification of Wave131-YFP fluorescence intensity in control, after gravity stimulation and after NAA application. Wave131-YFP fluorescence intensity was measured independently in outer and inner endodermis cell sides of upper and lower sides of hypocotyl. Graph represents percentage of Wave131-YFP fluorescence intensity for independent endodermis cell sides after independent treatments. Data do not show any significant difference compared to the control.

(E) Relative PIN3-GFP fluorescent signal at the outer and inner lateral endodermis cell sides of the left/upper and right/lower hypocotyl sides. The measurements were done in the same focal plane. Units are arbitrary fluorescence units (AU). Independently measured PIN3-GFP fluorescence intensity shows depletion of PIN3-GFP from the outer side of endodermal cells after 4 h of NAA treatment or from the outer upper endodermal cell side after 6 h of gravistimulation. Graph shows mean signal intensity separately for independent endodermal cell sides in hypocotyls. Error bars represent standard errors (Student's t test, ** $P < 0.01$).

(F and G) No altered PIN3-GFP localization in the hypocotyl endodermis when treated on plates supplemented with cychloheximide (CHX) (F). Cotreatment of CHX with NAA showed higher sensitivity in auxin-mediated PIN3-GFP inner-lateralization in endodermal cells (G).

(H) Graph shows mean ratio of inner-to-outer signal intensity for the indicated treatments. Error bars represent standard errors (Student's *t* test, * $P < 0.05$; ** $P < 0.001$; *** $P < 0.001$).

(I-K) No altered PIN3-GFP localization in the hypocotyl endodermis was observed when grown on plates supplemented with MG132 (I). MG132/NAA cotreatment showed a reduction

in PIN3-GFP inner-lateralization as compared to NAA treatment alone (I). Arrowheads point to PIN3 depletion from the outer-lateral side of endodermal cells. (K) Quantitative evaluation of auxin-dependent PIN3-GFP polarization in endodermal cells. Graph shows mean ratio of inner-to-outer signal intensity for the indicated treatments. Error bars are standard errors (Student's *t* test: * $P < 0.05$; ** $P < 0.01$).

(L-Q) No inhibition of the hypocotyl gravity response when treated with wortmannin (WM) (M) compared to DMSO control (L). Graph shows no gravity bending defects upon treatment with WM at the indicated concentrations (N). Gravity-induced PIN3-GFP polarization in hypocotyls after WM pretreatment followed with gravity stimulation (P). DMSO-treated control (O). Graph shows the mean ratio of lower-to-upper PIN3-GFP fluorescence intensities in endodermis cells in the outer endodermis cell sides (Q). Error bars are standard errors (Student's *t* test: * $P<0.05$; ** $P<0.01$).

Figure S4 (Related to Figure 3 and Figure 4)

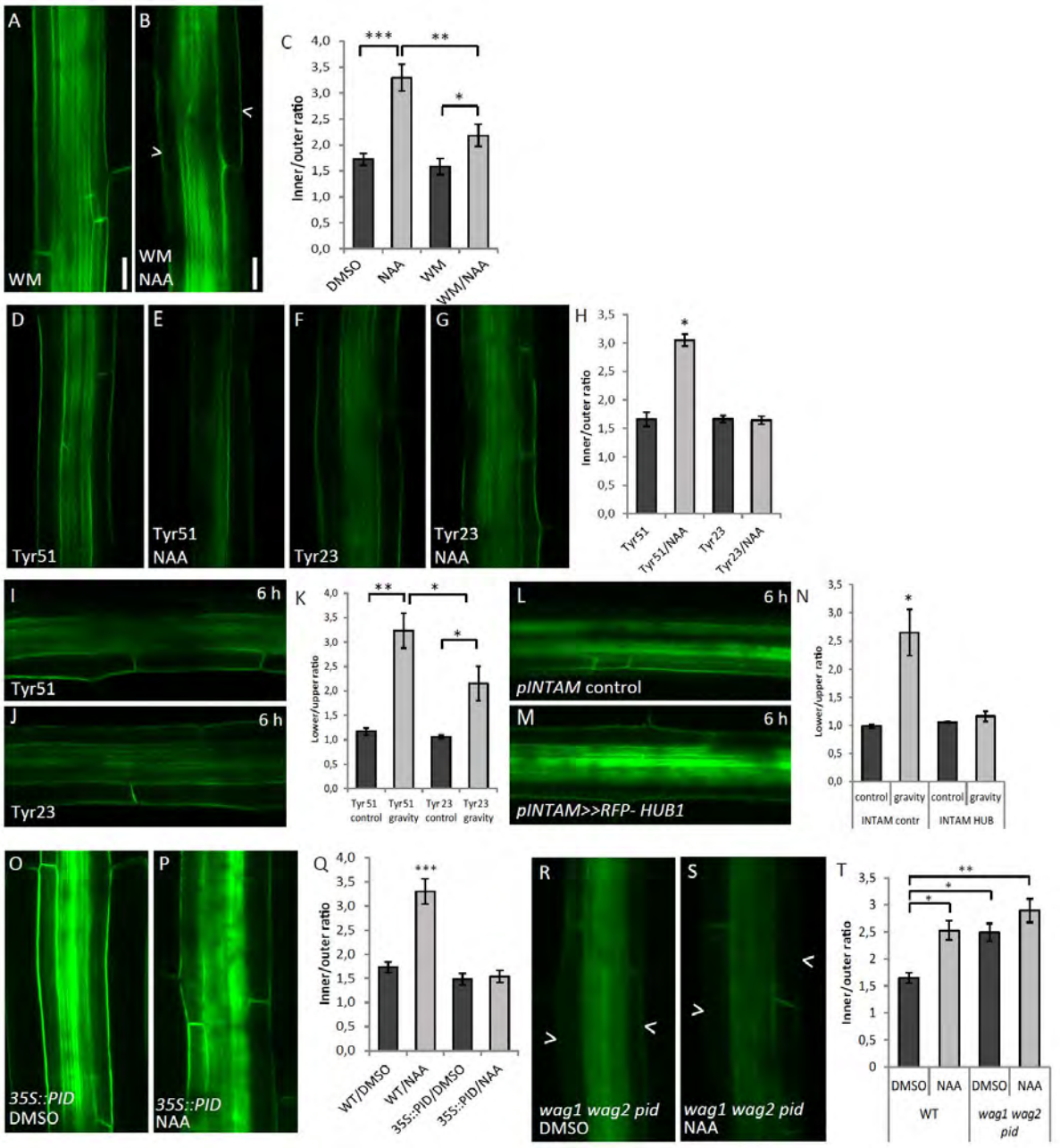

Figure S4. Clathrin-mediated endocytosis and PINOID-mediated phosphorylation during gravity- and auxin-mediated PIN3 polarity changes

(A-C) Auxin-induced PIN3-GFP polarization was partially inhibited by WM/NAA cotreatment (B) compared to the control treated with WM alone (A). (C) Quantitative evaluation of auxin-dependent PIN3-GFP polarization in endodermis cells. Graph shows mean ratio of inner-to-

outer signal intensity. Error bars represent standard errors (Student's *t* test, * P < 0.05; ** P < 0.01; *** P < 0.001).

(D-H) Unaffected steady-state PIN3 apolar localization by inhibition of clathrin-mediated endocytosis, shown by treatment with tyrphostin A23 (Tyr23) (F) compared to the inactive analog tyrphostin A51 (Tyr51) as control (D). Auxin-induced PIN3-GFP inner-lateralization was inhibited by Tyr23 (G), but not by Tyr51 (E). (H) Quantitative evaluation of auxin-dependent PIN3-GFP polarization in endodermis cells. Graph shows mean ratio of inner-to-outer signal intensity. Error bars represent standard errors (Student's *t* test, * P < 0.05).

(I-K) Tyr23 (J) effect on PIN3-GFP gravity-induced polarization in endodermal hypocotyl cells compared to that of its inactive analog Tyr51 (I). (K) Graph displays the mean ratio of the lower-to-upper PIN3-GFP fluorescence intensity at the outer PM of endodermis cells after gravity stimulation on Tyr23 and Tyr51 as negative control. Error bars are standard errors (Student's *t*-test, * P < 0.05; ** P < 0.01).

(L-N) *pINTAM>>RFP-HUB1* showing inhibition of PIN3-GFP polarization after gravity stimulation (M) compared to the control *pINTAM* (L). Before the experiment, lines were induced overnight with 2 μM tamoxifen. (N) Graph displays the mean ratio of the lower-to-upper PIN3-GFP fluorescence intensity at the outer endodermis PM after gravity stimulation. Error bars represent standard errors (Student's *t* test, * P < 0.05).

(O-Q) Overexpression of PID protein kinase in *35S::PID* leading to inhibition of the auxin-induced PIN3-GFP inner-lateralization (P) in hypocotyls compared to the untreated *35S::PID* hypocotyls (O). (Q) Quantitative evaluation of auxin-dependent PIN3-GFP polarization in endodermis cells. Graph shows mean ratio of inner-to-outer signal intensity. Error bars represent standard errors (Student's *t* test, *** P < 0.001).

(R-T) Slightly more pronounced inner-lateralized PIN3-GFP in untreated (R) and NAA-treated (S) *wag1 wag2 pid* mutant hypocotyls. (T) Quantitative evaluation of auxin-dependent PIN3-

GFP polarization in endodermis cells. Graph shows mean ratio of inner-to-outer signal intensity. Error bars represent standard errors (Student's *t* test, * $P < 0.05$; ** $P < 0.01$). Arrowheads point to PIN3 depletion from the outer-lateral side of endodermal cells. Scale bars represent 20 μm.

SUPPLEMENTAL EXPERIMENTAL PROCEDURES

Plant material and growth conditions

Arabidopsis thaliana (L.) Heynh, accession Columbia, was used as plant material. Published transgenic and mutant lines were used: *pPIN3::PIN3-GFP* [S1], *pPIN7::PIN7-GFP* [S2], *pSCR::PIN3-YFP* [S3], *pSCR::PIN2-GFP* [S4], *pUBQ10::Wave131-YFP* [S5], *pDR5rev::GFP* [S6], $GNOM^{M696L}$ [S7], *wag1 wag2 pid-14/+* [S8] (homozygous seedlings were selected based on the phenotype, not cotyledons in etiolated seedlings), *p35S::PID-21* [S9], *p35S::DII-VENUS* [S10], and *pINTAM>>RFP-HUB1* [S11] (before the experiment, lines were induced overnight with 2 µM of hydorxytamoxifen; Sigma-Aldrich), *PIN3::PIN3-GFP 35S::DII-VENUS* [S12]. *PIN3::PIN3-GFP* was introgressed in mutant backgrounds by crossing.

Plants were sown on half-strength Murashige and Skoog (½MS) plates with 1% (w/v) sucrose and 8 g/L agar (pH 5.8). Seeds were vernalized for 2 days at 4°C, exposed to light for 5-6 h at 18°C, and cultivated in the dark at 18°C or 21°C. For gravitropic stimulations, plates with 4-day-old etiolated seedlings were rotated 90°. The hypocotyls of *p35S::PID-21* were straightened up before the gravity stimulation. Seedlings were either scanned for measurements with ImageJ, analyzed by real-time phenotype analysis, or imaged by confocal microscopy. Each experiment was done at least in triplicate. For confocal microscopy, LSM 700 and LSM 800 confocal scanning microscopes (Zeiss, Germany) were used.

Real-time analysis

The gravity response of seedlings was recorded at 1- or 2-h intervals for 1 or 2 days at 18°C with an infrared light source (880 nm LED; Velleman, Belgium) by a spectrum-enhanced camera (EOS035 Canon Rebel Xti, 400DH) with built-in clear wideband-multicoated filter and standard accessories (Canon) and operated by the EOS utility software. Hypocotyls angles were

measured with ImageJ. Three replicates of at least 10 seedlings with a synchronized germination start were processed.

Quantitative analysis of DR5, DII-VENUS, and PIN3 polarization

Fluorescence intensity was measured in bent hypocotyl parts (Figure S1B, middle zone). The fluorescence intensity rate of *p35S::DII-VENUS* and *pDR5rev::GFP* was compared between the lower and upper sides of the hypocotyl in the responsive part as described previously [S3]. The signal ratio was calculated to circumvent the differential thickness of the hypocotyl tissue. For quantification of the gravity-induced PIN3-GFP polarization, the rate of the PIN3-GFP fluorescence intensity was compared between the outer PM sides of endodermal cells as described previously [S3]. The PIN3-GFP polarization was well visible in the upper endodermal cells, because the reduced cell signal was influenced with the PIN3-GFP signal in the stele.

The PIN3-GFP polarization was visible after 3 h of IAA treatment (Student's *t*-test; $P < 0.01$) and more pronounced after 4 h ($P < 0.001$) (Figures 2J). NAA treatment had a similar effect after 2 h ($P < 0.05$) and was more pronounced after 4 h ($P < 0.001$) when it reached the maximal effect (Figures S2A). Whereas already 1 μM IAA led to a significant polarization ($P < 0.05$), the effect of 10 μM IAA was more effective ($P< 0.001$) (Figure S2E). Similarly to IAA, 1 μM NAA led to a significant polarization ($P < 0.05$) that increased at 10 μM ($P < 0.001$) (Figures S2B).

For the auxin-induced PIN3-GFP polarization, the mean of the fluorescence intensity of the PIN3-GFP signal was measured at the inner-lateral and the outer-lateral membranes of endodermal cells. As control, the upper, middle, and lower parts of etiolated hypocotyls were compared for the auxin-mediated PIN3-GFP inner-lateralization. Cells in these three hypocotyl parts responded similarly. These data suggest that all the endodermal hypocotyl cells have the

potential to change the PIN3-GFP localization after NAA treatment, but that the gravity-induced bending takes place only in the upper part of hypocotyls [S3]. Therefore, the upper hypocotyl part was compared for its NAA response in case of different mutants and treatments. For the DII-VENUS, *pDR5::G/RFP*, and PIN3-GFP intensity measurements, the equivalent hypocotyl positions were used as controls.

For various time point quantifications (see Figures S1 and S3), the fluorescence intensity of the endodermal PM was measured in the bending side of hypocotyls (Figure S1B, middle). The differential PIN3-GFP/Wave131-YFP localization was presented as the percentage of the fluorescence intensity to overcome the low signal intensity in the lower hypocotyl parts due to the high hypocotyl thickness. For each time point, >10 hypocotyls/2 cell on each side (for PIN3-GFP >25 hypocotyls per each time point) were evaluated and the percentage was calculated individually for each time point from the average of the fluorescence intensity of the corresponding endodermis cell side.

All intensities were measured with ImageJ. Three replicates of at least 10 seedlings with a synchronized germination start were processed. The presented value is the mean of the averages. Student's *t* test was applied for statistic evaluation.

Pharmacological treatments

Treatments in the dark were done by transfer and incubation of 4-day-old etiolated *pPIN3::PIN3-GFP* seedlings on solid medium supplemented with NAA (10 μM; if not mentioned otherwise, Duchefa), IAA (10 μM; if not mentioned otherwise, Duchefa), brefeldin A (50 μM; Sigma), MG132 (25 μM, Calbiochem), wortmannin (30 μM; Sigma-Aldrich), cychloheximide (50 μM; Sigma-Aldrich), tyrphostin A23 (30 μM; Sigma-Aldrich), tyrphostin A51 (30 μM; Sigma-Aldrich), and NPA (10 μM; Sigma-Aldrich). All stock solutions are prepared in DMSO. All cotreatments with NAA were done after 1 h of pretreatment with the

drug followed by 4 h of cotreatment with NAA or 6 h of gravity stimulation. As standard auxin treatment condition, 10 μM NAA was used for 4 h. Control treatments contained an equivalent amount of solvent (DMSO; Sigma-Aldrich). Plants were grown first without chemicals, transferred for 1 h on chemical-containing solid medium prior to gravity stimulation or another transfer on medium containing chemical and NAA together. For the treatments during the gravitropic response, 3-day-old seedlings were germinated and grown on a mesh placed on the solid DMSO-containing medium and after the indicated time of gravity stimulation transferred with the mesh to medium containing NPA or Tyr23. As a parallel experiment, before gravity stimulation, 3-day-old seedlings were pretreated for 2 h with NPA for 8 h. Seedlings were transferred to the dark room with a dull red light. For all comparisons, at least three independent experiments were carried out with the same results.

SUPPLEMENTAL REFERENCES

S1. Žádníková, P., Petrášek, J., Marhavý, P., Raz, V., Vandenbussche, F., Ding, Z., Schwarzerová, K., Morita, M.T., Tasaka, M., Hejátko, J., et al. (2010). Role of PIN-mediated auxin efflux in apical hook development of *Arabidopsis thaliana*. Development *137*, 607-617.

S2. Blilou, I., Xu, J., Wildwater, M., Willemsen, V., Paponov, I., Friml, J., Heidstra, R., Aida, M., Palme, K., and Scheres, B. (2005). The PIN auxin efflux facilitator network controls growth and patterning in *Arabidopsis* roots. Nature *433*, 39-44.

S3. Rakusová, H., Gallego-Bartolome, J., Vanstraelen, M., Robert, H.S., Alabadi, D., Blazquez, M.A., Benková, E., and Friml, J. (2011). Polarization of PIN3-dependent auxin transport for hypocotyl gravitropic response in *Arabidopsis thaliana*. Plant J. *67*, 817-826.

S4. Xu, J., Hofhuis, H., Heidstra, R., Sauer, M., Friml, J., and Scheres, B. (2006). A molecular framework for plant regeneration. Science *311*, 385-388.

S5. Geldner, N., Denervaud-Tendon, V., Hyman, D.L., Mayer, U., Stierhof, Y.-D., and Chory, J. (2009). Rapid, combinatorial analysis of membrane compartments in intact plants with a multicolor marker set. Plant J. *59*, 169-178.

S6. Friml, J., Vieten, A., Sauer, M., Weijers, D., Schwarz, H., Hamann, T., Offringa, R., and Jürgens, G. (2003). Efflux-dependent auxin gradients establish the apical-basal axis of *Arabidopsis*. Nature *426*, 147-153.

S7. Geldner, N., Anders, N., Wolters, H., Keicher, J., Kornberger, W., Muller, P., Delbarre, A., Ueda, T., Nakano, A., and Jürgens, G. (2003). The *Arabidopsis* GNOM ARF-GEF mediates endosomal recycling, auxin transport, and auxin-dependent plant growth. Cell *112*, 219-230.

S8. Dhonukshe, P., Huang, F., Galvan-Ampudia, C.S., Mähönen, A.P., Kleine-Vehn, J., Xu, J., Quint, A., Prasad, K., Friml, J., Scheres, B., et al. (2010). Plasma membrane-bound AGC3 kinases phosphorylate PIN auxin carriers at TPRXS(N/S) motifs to direct apical PIN recycling. Development *137*, 3245-3255.

S9. Benjamins, R., Quint, A., Weijers, D., Hooykaas, P., and Offringa, R. (2001). The PINOID protein kinase regulates organ development in *Arabidopsis* by enhancing polar auxin transport. Development *128*, 4057-4067.

S10. Brunoud, G., Wells, D.M., Oliva, M., Larrieu, A., Mirabet, V., Burrow, A.H., Beeckman, T., Kepinski, S., Traas, J., Bennett, M.J., and Vernoux, T. (2012). A novel sensor to map auxin response and distribution at high spatio-temporal resolution. Nature *482*, 103-106.

S11. Robert, S., Kleine-Vehn, J., Barbez, E., Sauer, M., Paciorek, T., Baster, P., Vanneste, S., Zhang, J., Simon, S., Čovanová, M., et al. (2010). ABP1 mediates auxin inhibition of clathrin-dependent endocytosis in *Arabidopsis*. Cell *143*, 111-121.

S12. Le, J., Liu, X.-G., Yang, K.-Z., Chen, X.-L., Zou, J.-J., Wang, H.-Z., Wang, M., Vanneste, S., Morita, M., Tasaka, M., et al. (2014). Auxin transport and activity regulate stomatal patterning and development. Nat. Commun. *5*, 3090.